

Document downloaded from:

<http://hdl.handle.net/10251/193323>

This paper must be cited as:

Gil-Castell, O.; Teruel-Juanes, R.; Arenga, F.; Salaberria, AM.; Baschetti, M.; Labidi, J.; Badia, J.... (2019). Crosslinked chitosan/poly(vinyl alcohol)-based polyelectrolytes for proton exchange membranes. *Reactive and Functional Polymers*. 142:213-222.
<https://doi.org/10.1016/j.reactfunctpolym.2019.06.003>



The final publication is available at

<https://doi.org/10.1016/j.reactfunctpolym.2019.06.003>

Copyright Elsevier

Additional Information

Crosslinked chitosan/poly(vinyl alcohol)-based polyelectrolytes for proton exchange membranes

O. Gil-Castell¹, R. Teruel-Juanes¹, F. Arenga^{1,2}, A. M. Salaberria³, M. G. Baschetti², J. Labidi³, J. D. Badia^{1,4}, A. Ribes-Greus^{1,*}

This is an open-access version, according to <http://sherpa.ac.uk/romeo/issn/1381-5148/es/>

Full text available at: <https://www.sciencedirect.com/science/article/pii/S1381514819302925>

DOI: <https://doi.org/10.1016/j.reactfunctpolym.2019.06.003>

Please, cite it as:

O. Gil-Castell, R. Teruel-Juanes, F. Arenga, A. M. Salaberria, M. G. Baschetti, J. Labidi, J. D. Badia, A. Ribes-Greus. Crosslinked chitosan/poly(vinyl alcohol)-based polyelectrolytes for proton exchange membranes. *Reactive and Functional Polymers* 2019:142:213-222

¹Instituto de Tecnología de Materiales (ITM). Universitat Politècnica de València. Camino de Vera s/n, 46022 Valencia, Spain.

²Dipartimento di Ingegneria Civile, Chimica, Ambientale e dei Materiali (DICAM), Alma Mater Studiorum – Università di Bologna. Via Terracini, 28, 40131, Bologna, Italy.

³Department of Chemical and Environmental Engineering. University of the Basque Country. Plaza Europa 1, 20018, San Sebastián, Spain.

⁴Department of Chemical Engineering. School of Engineering. Universitat de València. Av. de la Universitat, s/n, 46100, Burjassot, Spain.

*Corresponding author:

A. Ribes-Greus aribes@ter.upv.es

Crosslinked chitosan/poly(vinyl alcohol)-based polyelectrolytes for proton exchange membranes

O. Gil-Castell¹, R. Teruel-Juanes¹, F. Arenga^{1,2}, A. M. Salaberria³, M. G. Baschetti², J. Labidi³, J. D. Badia^{1,4}, A. Ribes-Greus^{1,*}

Abstract

The preparation polyelectrolytes based on crosslinked poly(vinyl alcohol) (PVA) and chitosan (CS) was considered as a feasible alternative to develop highly functionalised, cost-effective and eco-friendly membranes for proton exchange fuel cell technologies. CS/PVA-based membranes were combined with sulfosuccinic acid (SSA) as crosslinking and sulfonating agent, and glycerol (GL) to promote flexibility and favour their manageability. The chemical structure, the thermo-oxidative behaviour, the ethanol uptake, the electric, the proton conductivity, and the performance in direct ethanol fuel cell (DEFC) were assessed. In general, all the CS/PVA-based polyelectrolytes showed a synergetic increase of thermo-oxidative stability, appropriate absorption and diffusion of ethanol and good proton conductivity, suitable for the typical service conditions of fuel cells. The GL in the membranes reacted with SSA, reduced the ethanol absorption, diffusion coefficient and proton conductivity, but acted as a plasticiser that increased the ductile manageability of the polyelectrolytes to be mounted on the membrane-electrode assembly (MEA). Higher presence of CS and higher the proportion of GL in the polyelectrolyte, improved the material performance in the DEFC. In particular, the crosslinked polyelectrolyte 40CS/PVA/SSA/20GL with a 40 %wt. of CS referred to PVA, and a 20 %wt. of GL referred to CS, showed a suitable behaviour in the DEFC test, with a maximum value of power density of 746 mW·cm⁻².

Keywords

Polyelectrolyte; proton exchange membrane; direct ethanol fuel cell (DEFC); poly(vinyl alcohol) (PVA); chitosan (CS)

1. Introduction

A proton exchange fuel cell (PEFC) is a promising power generation system that converts the chemical energy of hydrogen or bio-alcohols into electricity through an electrochemical reaction [1]. Although the fuel cell technology has substantially matured over the past decades, technological barriers, such as the cost of the fuel cell components –polyelectrolyte, catalysers, electrodes– or the hydrogen management –storage, transport and infrastructure– still delay their massive implantation and commercialisation [2]. Nafion®, as the most common and commercially available polymer electrolyte membrane (PEM), possess ideal properties for being used with hydrogen, such as high proton conductivity and good chemical, mechanical, and thermal stability. However, Nafion®-based membranes have several intrinsic disadvantages, such as a high cost, high permeability to alcohols, or instability and dehydration at temperatures above 80 °C [3].

In recent years, there has been an extensive research on the development of high performance, cost-effective and eco-friendly polymer electrolytes. Among the novel proposed materials, the biomass-derived resources have received great attention [4]. In this context, chitosan (CS), the *N*-deacetylated derivative of chitin (CH), is one of the promising candidates. It is hydrophilic and insoluble in water, alkali and organic solvents. Its solubility in diluted organic acids allows for the gel formation in various configurations [5]. Free amine and hydroxyl functional groups on the CS backbone enable various chemical modifications to tailor it for specific applications [6]. Thus, CS is a potentially useful bio-based material for PEMs due to their renewable origin –can easily be obtained from crabs or shrimp shells and fungal mycelia–, suitable properties, high availability, low cost and low permeability to alcohols [7,8]. However, in its native state, CS exhibits very low proton conductivity and high degrees of swelling [9]. To address these issues, CS is usually either ionized and crosslinked [10], reinforced [11], or blended with other polymers [7].

Chitosan-based blends with poly(acrylic acid) (PAA), poly(ether sulfone) (PES) or poly(vinyl alcohol) (PVA) are a feasible alternative to improve the performance for PEMs [12–16]. In particular, CS and PVA are reasonably compatible due the strong hydrogen bonding interaction between the amine and hydroxyl groups [17,18]. The crosslinking of the blend is a feasible mode to obtain three-dimensional networks, improve dimensional stability, thermal and mechanical properties, reduce the ethanol permeability and enhance proton conductivity [15,19]. Although crosslinking agents such as glutaraldehyde have been proposed [20], interesting results have been obtained using sulfosuccinic acid (SSA) in the field of fuel cells, since it brings negative charged ions to the blend structure. In particular, the effect of the percentage of SSA in a 1:1 PVA/CS blends has been reported by *Witt et al.* [21]. Therefore, a step forward would be the evaluation of the variation of the PVA to CS proportion in the blend.

In the present work, crosslinked CS/PVA blended polyelectrolytes were considered, containing sulfosuccinic acid (SSA) as crosslinking and sulfonating agent to enhance the proton conductivity, and glycerol (GL) to endorse plasticity to the membranes. The combined assessment of the chemical stability, the thermo-oxidative behaviour, the ethanol absorption profiles, the electric and the proton conductivity along with the power density was proposed as a suitable validation methodology. The present approach might help design successfully alternative polyelectrolytes for direct ethanol fuel cells (DEFC).

2. Materials and methods

2.1. Materials

Chitosan (CS) with an average molar mass in number (M_n) in the range from 50000 to 190000 g·mol⁻¹, poly(vinyl alcohol) (PVA) with M_n 130000 g·mol⁻¹ (degree of hydrolysis min. 99%), glacial acetic acid (99.8% anhydrous), sulfosuccinic acid (SSA) (70 %wt. solution in water) and glycerol (≥99.5%) were all purchased from Sigma-Aldrich.

2.2. Membrane preparation

The chitosan/poly(vinyl alcohol) blends (CS/PVA) were prepared by means of a joint solvent-casting/crosslinking procedure. For this purpose, an 8 %wt. PVA solution was prepared in deionised water and left into a reflux system at 90 °C for 6 h under magnetic stirring. The concentration of the CS solution was fixed at 2 %wt. in diluted acetic acid and was left to dissolve under magnetic stirring at room temperature for 6 h. The PVA/CS blends were obtained by mixing and homogenising the CS and PVA solutions at 65 °C under magnetic stirring for 16 h.

In order to improve the plasticity of the membranes, glycerol (GL) was added to the CS/PVA blends in 10 and 20 %wt. in relation to CS. To achieve crosslinking and functionalisation, sulfosuccinic acid (SSA) was added to the mixture in a 30 %wt. in relation to PVA and homogenized under magnetic stirring for 30 min [22].

For the membrane preparation, the homogeneous solutions were poured into Teflon® moulds and the cast films were allowed to dry at room temperature for 48 h. Then, they were peeled off the Teflon® plates and crosslinked by thermo-compression into a hydraulic hot plates press at 110 °C for 2 h. For this purpose, the films were introduced into a Teflon® mould of 50 µm thickness and, in turn, between of fiberglass reinforced Teflon® sheets. Once elapsed the crosslinking time, the mould assembly was cooled at room temperature. Finally, all the membranes were kept into zip bags and stored into a desiccator for further analyses.

In the following, the different materials will be identified as x CS/PVA/SSA/ y GL, where x is the weight percentage of CS referred to PVA and y is the weight percentage of GL in relation to CS. The nomenclature of each membrane and the real experimental blending composition, taking into account all the components contained in the membrane, are shown in **Table 1**. Pure CS and PVA/SSA were considered as references. Compositions with a concentration of CS higher than 55% resulted in unmanageable membranes due to its massive rigidity, and were not further considered in this study.

Table 1. Nomenclature and experimental composition of CS/PVA-based polyelectrolytes.

Membrane	CS (% wt.)	PVA (% wt.)	SSA (% wt.PVA)	GL (%wt.CS)
CS	100	-	-	-
60CS/PVA/SSA	53.57	35.71	10.71	-
50CS/PVA/SSA	43.48	43.48	13.04	-
40CS/PVA/SSA	33.90	50.85	15.25	-
20CS/PVA/SSA	16.13	64.52	19.35	-
PVA/SSA	-	76.92	23.08	-
60CS/PVA/SSA/10GL	50.85	33.90	10.17	5.08
50CS/PVA/SSA/10GL	41.67	41.67	12.50	4.16
40CS/PVA/SSA/10GL	32.80	49.18	14.75	3.27
20CS/PVA/SSA/10GL	15.88	63.49	19.05	1.58
PVA/SSA/10GL	-	71.43	21.43	7.14
60CS/PVA/SSA/20GL	50.00	33.33	10.00	6.67
50CS/PVA/SSA/20GL	40.00	40.00	12.00	8.00
40CS/PVA/SSA/20GL	30.77	46.15	13.84	9.23
20CS/PVA/SSA/20GL	14.29	57.14	17.14	11.43
PVA/SSA/20GL	-	66.67	20.00	13.33

2.3. Membrane characterisation

2.3.1. Fourier transform infrared spectroscopy (FT-IR)

The Fourier transform infrared spectroscopy (FTIR) analysis was performed using a Thermo Nicolet 5700 FT-IR spectrometer. The FTIR spectra were collected in the range from 4000 to 400 cm^{-1} using the Attenuated Total Reflectance (ATR) mode at a resolution of 4 cm^{-1} . In order to obtain accurate results, 64 scans were performed at three different locations of the sample and the average was calculated. Backgrounds spectra were collected before each series of experiments in order to eliminate any interference from the environment. Results were processed by means of the Omnic® Software.

2.3.2. Thermogravimetric analysis (TGA)

The thermogravimetric analysis (TGA) was performed using a Mettler Toledo TGA/STDA 851 analyser. The samples, with a mass between 3 and 5 mg, were filled into 70 μL alumina capsules. Then, they were analysed under a dynamic segment with a heating rate of 10 $^{\circ}\text{C}\cdot\text{min}^{-1}$ from 30 to 700 $^{\circ}\text{C}$ and oxidative atmosphere of O_2 at 50 $\text{mL}\cdot\text{min}^{-1}$. The samples were assessed in triplicates and the averages of results were taken as representative values. Data were evaluated by means of the STARe® Software.

2.3.3. Ethanol solution uptake

The absorption of ethanol solution was studied to understand membrane wettability in condition close to normal DEFC and was evaluated by performing swelling tests on the CS/PVA/SSA-based membranes. Samples were cut into rectangular specimens and dried 12 h at 30 $^{\circ}\text{C}$ in a vacuum oven Heraeus Vacutherm, in order to ensure the elimination of humidity. Then, the samples were immersed into a 2 M ethanol solution and subjected to 40 $^{\circ}\text{C}$. The sorption measurements consisted in removing the sample from the solution, blotting the surface free of liquid, immediately weighing the sample on a Mettler Toledo model XS105 scale with a precision of

0.01 mg, and then re-immersing the membranes into a fresh 2 M ethanol solution. This process was repeated many times over a short time interval between 30 min and 2 h. Then, the time interval was extended to 4, 8, 12 and 24 h until no further gain weight was observed and equilibrium wet mass (M_{eq}) was reached. The variation of the sample mass due to the solution absorption (M_t) was calculated according to **Equation 1**.

$$M_t = \frac{m_t - m_0}{m_0} \times 100 \quad \text{(Equation 1)}$$

Where m_t is the mass during ethanol solution absorption and m_0 is the mass at the beginning.

The solution to Fick's law for diffusion is different depending on the geometric structure of the material under study [23]. For a plane sheet geometry, as that of the obtained membranes, if the mass uptake at time t is used as M_t and the uptake at the equilibrium as M_{eq} , the Fick's law can be simplified using Stefan's approximation (**Equation 2**). This estimation is used for describing the earlier stages of uptake, usually for $M_t/M_S \leq 0.5$.

$$\frac{M_t}{M_{eq}} = \frac{8}{\pi^{1/2}} \left(\frac{Dt}{l^2} \right)^{1/2} \quad \text{(Equation 2)}$$

Where D is the diffusion coefficient, t the time of absorption and l is the thickness of the sample that was evaluated using a micrometre Mitutoyo Comparator Stand 215-611 BS-10M and taking the average of six measurements in different positions of the sample. If the semi-saturation time ($t_{1/2}$) is considered when $\frac{M_t}{M_{eq}} = 0.5$, the **Equation 2** could be expressed as **Equation 3**.

$$t_{1/2} \approx \frac{\pi}{256} \cdot \left(\frac{l^2}{D} \right) \quad \text{(Equation 3)}$$

Which in turn, finally results in **Equation 4** for the calculation of D that can be used in the present work to assess the effective diffusion coefficient of the ethanol solution in the different materials.

$$D \approx 0.01224 \frac{l^2}{t_{1/2}} \quad \text{(Equation 4)}$$

2.3.4. Dielectric-thermal impedance spectrometry

The impedance measurements were performed using the Novocontrol Broadband Dielectric Impedance Spectrometer (BDIS) equipment connected to a Novocontrol Alpha-A Frequency Response Analyser. A BDS-1200 Novocontrol parallel-plated capacitor with two plated electrodes was used as dielectric cell test. Next, the analyses consisted in a single sweep at room temperature (25 ± 1 °C) in a frequency range from 10^{-2} to 10^7 Hz.

The proton conductivity of the CS/PVA-based polyelectrolytes was calculated according to the **Equation 5**.

$$\sigma_{prot} = \frac{l}{A \cdot R_0} \quad \text{(Equation 5)}$$

where l is once again the thickness of the CS/PVA-based polyelectrolytes in cm, A the area of the electrode in contact with the membrane in cm^2 , and R_0 the protonic resistance in Ohm (Ω). The value of R_0 is taken from the Bode plot in the high frequencies range, in which the value of $\log |Z|$

tends to a non-frequency dependent asymptotic value and the phase angle reaches its maximum value [24].

The electric conductivity (σ_{elec}) was measured at low frequencies, where the measured real part of the conductivity (σ') reaches a plateau, that is correlated to the DC conductivity (σ_0).

2.3.5. Direct ethanol fuel cell (DEFC) test

The direct ethanol fuel cell (DEFC) performance tests were conducted into a single cell F-107 from H-TEC with diffusing layers. The membranes were previously equilibrated with a 2 M ethanol solution during 24 h to ensure their fully hydrated state, and were sandwiched between two electrode catalyst sheets of platinum (Pt). The active area of the single cell was approximately $4 \times 4 \text{ cm}^2$. The gas flow rates of the 2 M ethanol solution as fuel and oxidant humid air stream were kept constant at $0.250 \text{ L} \cdot \text{min}^{-1}$ and $1.6 \text{ L} \cdot \text{min}^{-1}$, respectively.

3. Results and discussion

3.1. Physico-chemical characterisation of the membranes: macroscopic appearance, chemical structure and thermo-oxidative stability

The macroscopic appearance of all the crosslinked membranes is shown in **Figure 1**. In general, a flat morphology with uniform surface with a thickness between 35 and 55 μm was achieved. All the polyelectrolytes, initially transparent, experienced a change of colour after crosslinking. This change was more pronounced for those with higher content of PVA, which corroborated the crosslinking reaction with the SSA molecules. During manipulation, the crosslinked membranes were rigid. However, those containing glycerol (GL) were more flexible and handily.

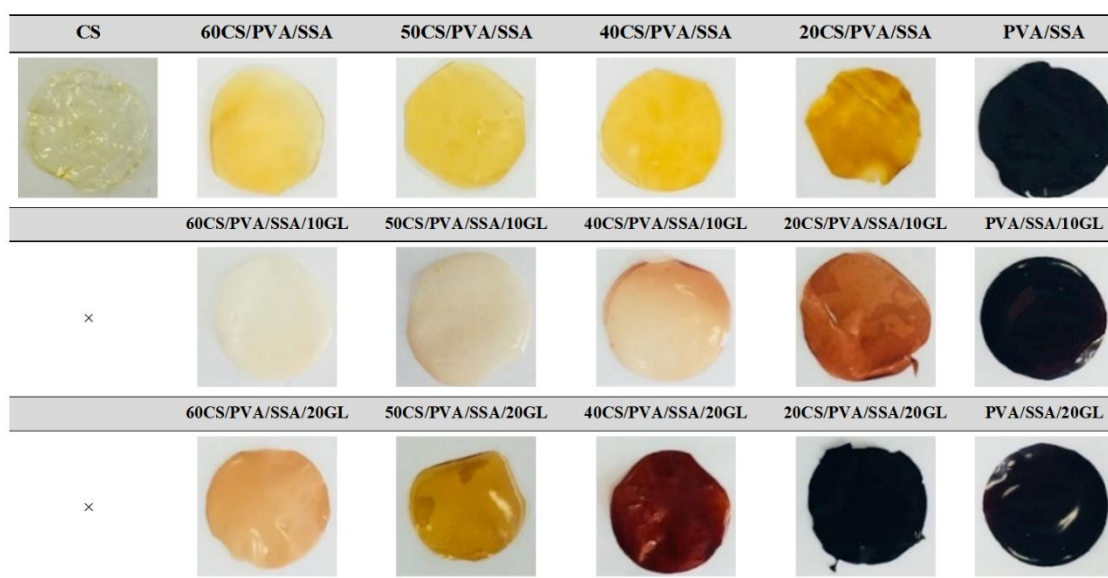


Figure 1. Macroscopic appearance of the CS/PVA-based crosslinked polyelectrolytes.

Fourier transform infrared spectroscopy (FTIR) was carried out in order to assess the blending, the crosslinking reaction of CS/PVA with the SSA molecules and the effect of the addition of GL. The obtained spectra are plotted in **Figure 2**. Neat CS and crosslinked PVA/SSA were taken as references.

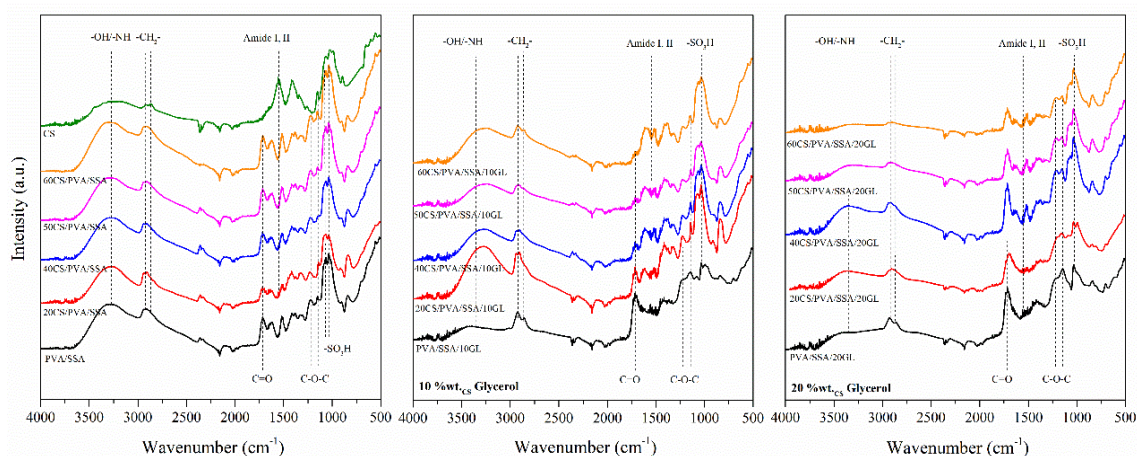


Figure 2. FTIR spectra of the crosslinked CS/PVA-based polyelectrolytes.

Briefly, the CS revealed a strong band in the region from 3200 to 3300 cm^{-1} due to the N–H and O–H stretching and intramolecular hydrogen bonds. Then, the symmetric and asymmetric stretching of the methylene groups C–H was perceived in the bands at 2950 and 2900 cm^{-1} , respectively. The vibrations at 1550 and 1470 cm^{-1} were assigned to the stretching of primary and secondary amides, respectively [25]. Finally, the bands at 1150 cm^{-1} associated to asymmetric stretching of the C–O–C bridge, and bands at 1060 and 1030 cm^{-1} due to the C–O stretching were found [26].

The PVA/SSA reference membrane revealed the –OH vibration broad band, as well as the methylene absorption bands in the range from 3500 to 2750 cm^{-1} . The crosslinking in this membrane was corroborated by the presence of the ester bonds by means of the C=O stretching vibration at 1720 cm^{-1} and the C–O–C absorption band at 1120 and 1240 cm^{-1} , respectively. The peaks at 1100–1030 cm^{-1} were associated with the symmetric stretching vibrations of the –SO₃H group introduced into the SSA molecules [27].

In general, the obtained spectra of the CS/PVA/SSA-based polyelectrolytes gathered the characteristic peaks of the components of the blend, including the signals of the CS, the PVA and the SSA. Indeed, the –OH stretching vibration in the PVA and the –NH stretching vibration in the CS were found, as well as the characteristic absorption bands for the methylene groups (–CH₂–) of PVA and CS [28,29]. As expected, the changes in the percentages of the components of the membrane reverberated in the spectra as a variation of the band intensity of the specific groups. The crosslinking reaction was confirmed in all the membranes by means of the absorption bands of the ester bond found for the PVA/SSA reference. The membrane sulfonation was assessed and the presence of the sulfonic group introduced by the SSA was corroborated. Although the –SO₃H signals may overlap with the C–O stretching of CS, the intensity of the band of the sulfonic group in the blends was more intense.

The addition of GL to the CS/PVA/SSA-based polyelectrolytes was then evaluated. The GL promoted a widening of the –OH band between 3000 and 3500 cm^{-1} , which pointed out the different nature of the –OH groups in these polyelectrolytes. The interactions of GL within the CS, PVA and SSA resulted in a reduction of the overall peak intensity, especially in the fingerprint region, which proved the plasticising effect of GL [30].

The thermo-oxidative decomposition of the CS/PVA/SSA-based polyelectrolytes was investigated using thermogravimetric analysis (TGA) under oxidative atmosphere. **Figure 3** shows the obtained thermogravimetric (TG) and the first-order derivative (DTG) curves of all the membranes, compared with CS and crosslinked PVA/SSA. The **Table 2** summarises the mass-loss percentage along with the peak temperature of the DTG curves at the different decomposition stages.

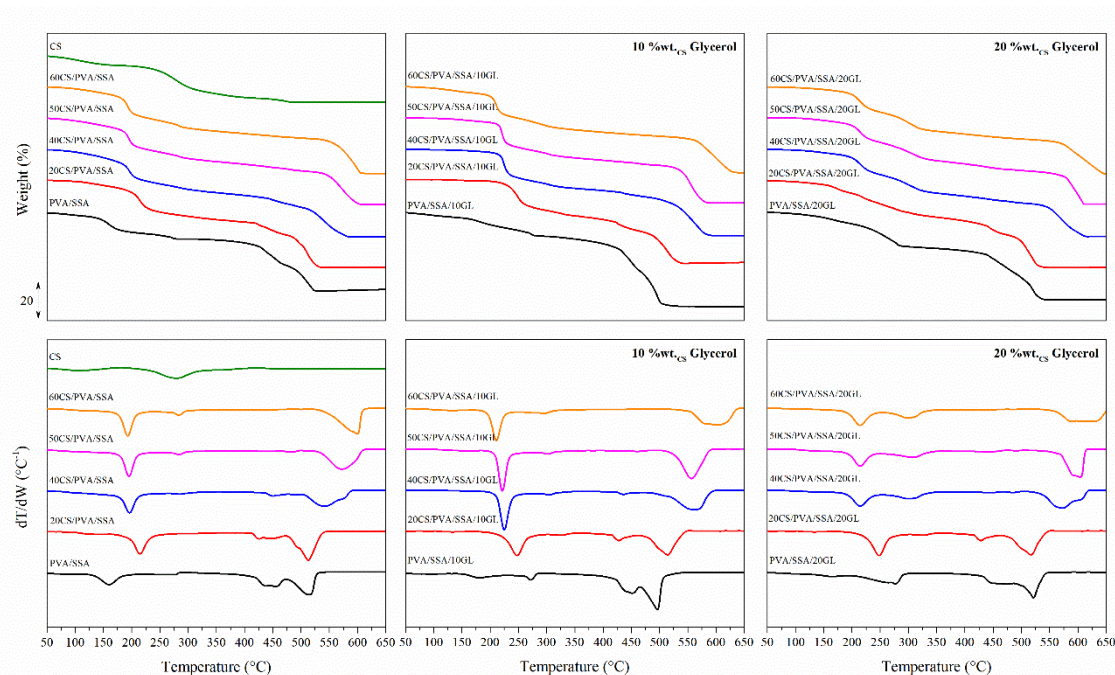


Figure 3. Thermogravimetric (TG) and derivative curves (DTG) of the CS/PVA-based polyelectrolytes.

The neat CS exhibited two main decomposition steps, around 104 °C and 280 °C, attributed to the loss of humidity and to the degradation of the polymer backbone, respectively [31,32]. The crosslinked PVA/SSA showed a multiple-stage thermo-oxidative process: (i) free and bound water release (50-250 °C); (ii) degradation of hydroxyl groups (250-300 °C) [33]; (iii) desulfonation process (400-475 °C); and (iv) degradation of the PVA backbone (475-650 °C).

In detail, the CS/PVA/SSA-based polyelectrolytes revealed the combined behaviour of their components [31–34]. The first stage, related to water release, moved towards lower temperatures as the CS percentage increased. Conversely, as PVA/SSA proportion increased in the membranes, the peak temperature of this stage was even higher than for the pure crosslinked PVA/SSA, which suggested a synergistic effect of CS, PVA and SSA, in terms of a strong interaction with water molecules. The mass-loss contribution of this stage was influenced by the membrane composition, being higher as the CS content increased. The hydrophilic nature of CS may be the responsible of higher humidity retention. The second stage corresponding to the decomposition of CS was also observed, with a mass-loss that increased when the CS percentage in the polyelectrolytes augmented, and corroborated the influence of the composition. The third stage was ascribed to the desulfonation processes and the breakdown of the crosslinking bond. This peak was more remarkable as the PVA/SSA percentage increased. Finally, the last stage associated to the breakage and decomposition of the PVA backbone by means of the chain-scission mechanism was observed, which moved to higher temperatures when CS content increased [15].

Although higher concentration of PVA/SSA would imply higher thermal stability given the higher crosslinking degree, the results showed the opposite trend. The hydrogen bonding interactions between the components is in part responsible for the structure stabilisation and, therefore, may determine the thermo-oxidative stability. The blended membranes with higher concentration of PVA/SSA have less free hydroxyl groups available for hydrogen bonding and consequently lower stability. In addition, as indicated by *Morancho and al.* [35], the catalysed elimination reactions of the hydroxyl groups under acidic conditions reduced the thermo-oxidative stability of the blends. The presence of acid traces from the crosslinking agent may also catalyse the decomposition.

The decomposition stage of GL between 200 and 300 °C was overlapped by the process previously ascribed to the bound water release, and was only perceivable in the neat crosslinked PVA/SSA (PVA/SSA/10GL and PVA/SSA/20GL). The addition of GL moved the water release process towards higher temperatures. The low molar mass molecules of GL may have modified the three-dimensional organization of the polymer matrix, occupying the available free volume [36,37]. As a result, stronger interactions between the CS, PVA, SSA and GL may reduce the humidity holding capability. The mass-loss associated to the water release stage decreased as the GL content increased in the membranes.

Table 2. Temperature peak (T) of the DTG curve along with the mass-loss (ΔW) of each stage during thermo-oxidative decomposition of the CS/PVA-based polyelectrolytes. Standard deviation lower than 3% was omitted for the sake of clarity.

Membrane	Water release		GL decomp.		CS decomp.		Desulfonation Crosslink decomp.			PVA decomp.	
	T_w (°C)	ΔW_w (%)	T_{GL} (°C)	ΔW_{GL} (%)	T_{CS} (°C)	ΔW_{CS} (%)	T_D (°C)	T_C (°C)	ΔW_{DC} (%)	T_{PVA} (°C)	ΔW_{PVA} (%)
CS	104.22	9.53	-	-	277.72	58.43	-	-	-	-	-
60CS/PVA/SSA	193.07	37.41	-	-	283.23	13.77	-	-	-	599.63	38.57
50CS/PVA/SSA	195.21	37.40	-	-	283.88	12.89	-	499.95	7.80	572.51	36.27
40CS/PVA/SSA	196.18	37.34	-	-	285.73	12.23	450.36	508.08	16.59	540.96	27.48
20CS/PVA/SSA	214.70	34.56	-	-	-	-	426.22	443.94	30.56	512.68	26.86
PVA/SSA	160.25	10.22	-	-	-	-	441.35	452.08	15.53	510.09	61.97
60CS/PVA/SSA/10GL	210.99	35.69	-	-	295.64	13.97	-	-	4.10	602.25	40.45
50CS/PVA/SSA/10GL	221.69	33.22	-	-	302.14	12.83	460.74	-	5.83	556.22	41.47
40CS/PVA/SSA/10GL	225.15	32.56	-	-	304.21	12.51	436.64	-	9.35	564.00	39.74
20CS/PVA/SSA/10GL	247.68	27.48	-	-	325.75	17.97	428.00	-	23.36	514.34	20.99
PVA/SSA/10GL	180.61	19.74	271.77	11.10	-	-	443.69	451.45	20.87	496.17	49.11
60CS/PVA/SSA/20GL	214.30	26.28	-	-	298.38	24.04	-	-	5.21	587.62	39.21
50CS/PVA/SSA/20GL	214.45	27.55	-	-	306.73	23.58	475.70	-	7.03	617.86	37.14
40CS/PVA/SSA/20GL	214.52	28.21	-	-	299.56	23.55	484.91	-	7.30	572.31	37.15
20CS/PVA/SSA/20GL	245.68	26.48	-	-	324.65	17.82	432.45	-	20.78	514.34	19.76
PVA/SSA/20GL	138.40	23.22	276.52	16.59	-	-	448.78	473.31	31.35	521.44	23.91

3.2. Ethanol solution uptake behaviour

The ethanol/water uptake behaviour was studied by means of the immersion of the polyelectrolytes into a 2 M ethanol aqueous solution at 40 °C. **Figure 4** shows the mass uptake at equilibrium for the CS/PVA/SSA and CS/PVA/SSA/GL-based polyelectrolytes as a function of the composition and the presence of GL in the membranes estimated from the experimental swelling curves.

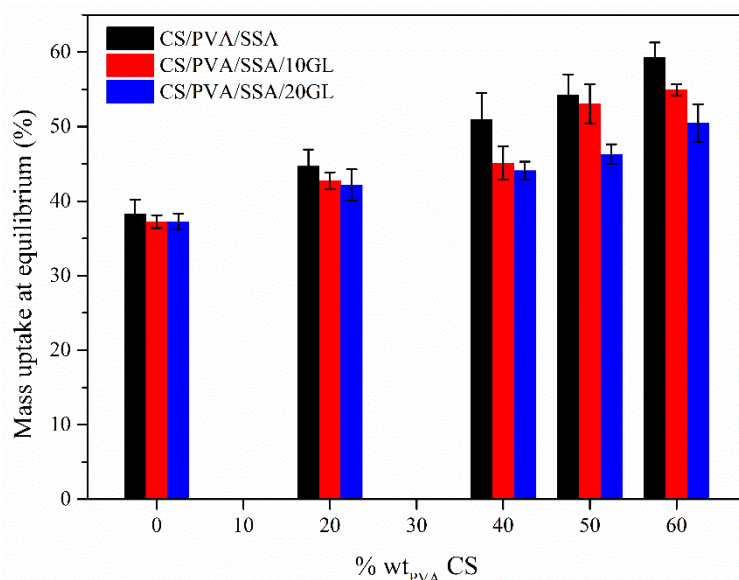


Figure 4. Mass uptake at equilibrium for the CS/PVA-based polyelectrolytes as a function of the CS composition and the GL content.

In general, the mass uptake at equilibrium was in the range between 35% and 60% for the crosslinked CS/PVA/SSA-based polyelectrolytes, which is essential for the application as fuel cell membranes and promote the vehicular proton transport mechanism [38–40]. Furthermore, no macroscopic deformations were observed, corroborating the high stability of the crosslinked membranes.

The uptake ability strongly depended on the CS and PVA ratio. In particular, the mass uptake at equilibrium increased with the CS percentage, which was attributed to the high water affinity of CS. Moreover, the membranes containing GL showed a decrease of the solution uptake. The plasticised membranes containing GL involved a more compact structure, which reduced the available sites for solution incorporation [37]. These results are in agreement with those found in the thermo-oxidative decomposition analyses, in which the CS enhanced the humidity retention and the addition of GL reduced the humidity content of the membranes.

The ethanol solution uptake was normalised between 0 and 1 for a better comparison of the saturation rates [41,42], which results are plotted in **Figure 5**. As well, the diffusion coefficient (D) was calculated by means of the **Equation 4**, which values are gathered in **Table 3**.

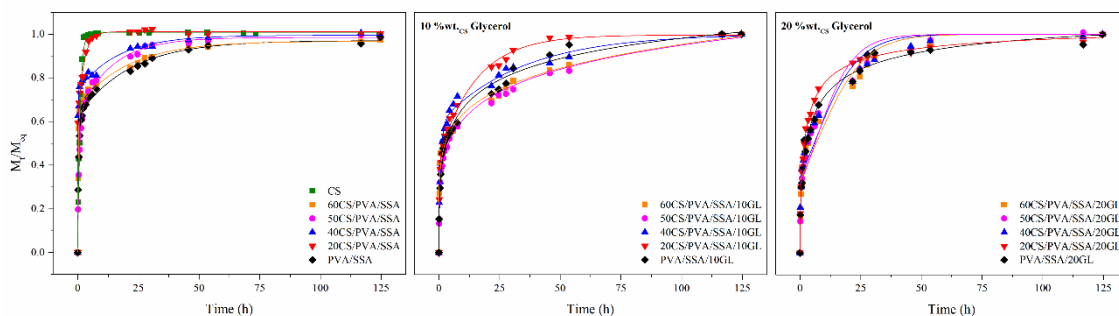


Figure 5. Normalised profiles of the ethanol solution uptake of the CS/PVA-based CS/PVA-based polyelectrolytes as a function of time.

Table 3. Diffusion coefficient (D) for the CS/PVA-based polyelectrolytes.

Membrane	$D \cdot 10^{10}$ ($\text{cm}^2 \cdot \text{s}^{-1}$)
CS	0.30
60CS/PVA/SSA	1.13
50CS/PVA/SSA	1.35
40CS/PVA/SSA	3.62
20CS/PVA/SSA	3.59
PVA/SSA	1.24
60CS/PVA/SSA/10GL	0.42
50CS/PVA/SSA/10GL	0.24
40CS/PVA/SSA/10GL	0.69
20CS/PVA/SSA/10GL	0.23
PVA/SSA/10GL	0.22
60CS/PVA/SSA/20GL	0.13
50CS/PVA/SSA/20GL	0.18
40CS/PVA/SSA/20GL	0.62
20CS/PVA/SSA/20GL	0.56
PVA/SSA/20GL	0.28

The highest absorption rates were obtained for the 40CS/PVA/SSA composition. This behaviour could be correlated to the high affinity of both materials CS and PVA to water. A strong reduction of the diffusion coefficient in the CS/PVASSA-based polyelectrolytes was observed as the percentage of GL increased. As suggested before, the strong interaction between the GL, CS and PVA decreased the absorption rate that prevents the membranes from excessive dimensional changes.

3.3. Electric and proton conductivity

The electric (σ_{elec}) and proton conductivity (σ_{prot}) of the polyelectrolyte are essential parameters that must be validated for fuel cell applications [43]. The electric conductivity (σ_{elec}) was considered at low frequencies, where the measured real part of the conductivity (σ') reaches a plateau that is correlated to the DC conductivity (σ_0), as shown in **Figure 6**. Given the intrinsic design of the proton exchange fuel cells, the electrical conductivity through the membranes must be avoided and, subsequently, high electrical resistance is required to promote the electronic flux in the external circuit. The obtained values are gathered in **Table 4**. In general, the σ_{elec} was found

around $10^{-8} \text{ S}\cdot\text{cm}^{-1}$ for all the developed CS/PVA/SSA-based polyelectrolytes, regardless the CS:PVA ratio or the amount of GL, which corroborated their performance as electric insulators [44].

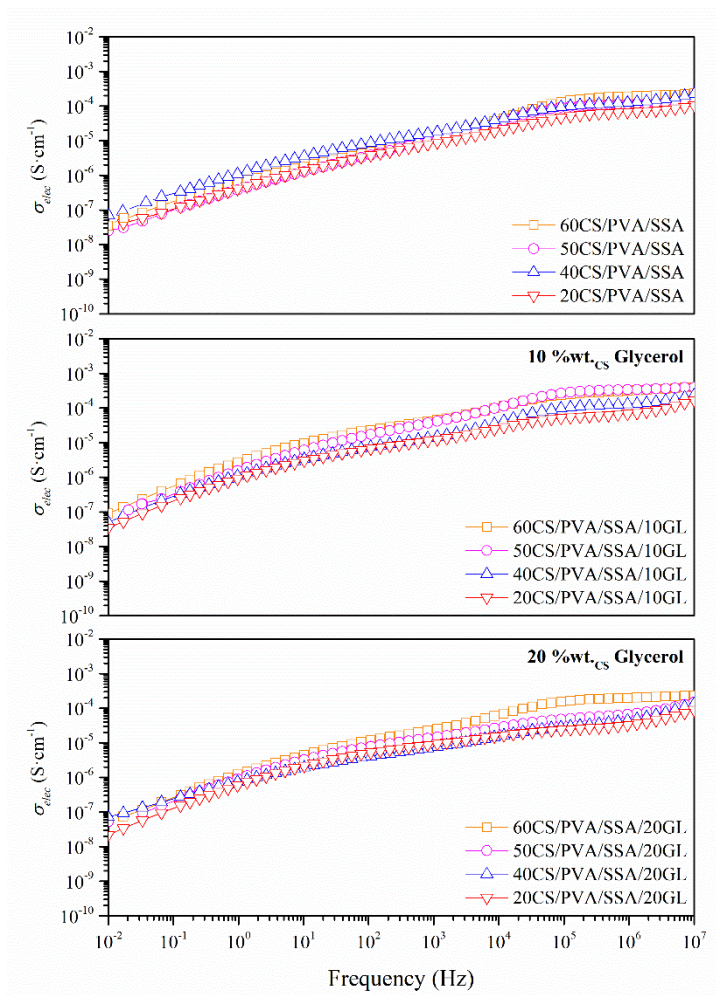


Figure 6. Electric conductivity (σ_{elec}) as a function of frequency of CS/PVA-based polyelectrolytes.

The proton conductivity (σ_{prot}) was assessed from the Bode diagrams, which were obtained from the impedance measurements at room temperature for the pre-hydrated CS/PVA-based polyelectrolytes. The resulting diagrams are plotted in **Figure 7** and the calculated σ_{prot} values are gathered in **Table 4**.

Table 4. Proton conductivity (σ_{prot}) and electric conductivity (σ_{elec}) for the pre-hydrated CS/PVA polyelectrolytes.

Membrane	$\sigma_{elec} \cdot 10^8$ ($S \cdot cm^{-1}$)	σ_{prot} ($mS \cdot cm^{-1}$)
60CS/PVA/SSA	5.36	0.246
50CS/PVA/SSA	2.50	0.225
40CS/PVA/SSA	6.85	0.735
20CS/PVA/SSA	3.65	0.285
60CS/PVA/SSA/10GL	9.07	0.112
50CS/PVA/SSA/10GL	5.84	0.118
40CS/PVA/SSA/10GL	5.01	0.151
20CS/PVA/SSA/10GL	3.45	0.106
60CS/PVA/SSA/20GL	3.98	0.186
50CS/PVA/SSA/20GL	5.24	0.120
40CS/PVA/SSA/20GL	7.25	0.189
20CS/PVA/SSA/20GL	2.17	0.190

In general, the blended crosslinked CS/PVA/SSA-based polyelectrolytes revealed higher proton conductivity in relation to pure CS, which presents a σ_{prot} of $0.011 \text{ mS} \cdot \text{cm}^{-1}$. The blending strategy, along with the crosslinking reaction with SSA, contributed to increase the proton conductivity of the membranes. The sulfonic acid groups ($-\text{SO}_3\text{H}$) of the SSA can be dissociated under hydrated conditions and act as proton carriers. The synergetic improvement of the blends gave rise to an equilibrated water absorption and retention ability, enabling easy proton transfer, in agreement with literature [45]. The observed values are still lower to that of the Nafion® membrane, endowed with a proton conductivity around $6 \text{ mS} \cdot \text{cm}^{-1}$ at $25 \text{ }^\circ\text{C}$ [15]. However, a significant improvement was observed if compared to CS and crosslinked PVA for the 40CS/PVA/SSA membrane, with a proton conductivity of $0.735 \text{ mS} \cdot \text{cm}^{-1}$.

As expected, when GL was added to the CS/PVA/SSA blends, a decrease in the proton conductivity was perceived. This trend was in close relation to the ethanol solution uptake measurements, which confirmed the essential relationship between the proton conductivity and the swelling ability. However, one may bear in mind the importance of GL in terms of processability, dimensional stability and therefore solutions of compromise must be found for the design of polyelectrolytes.

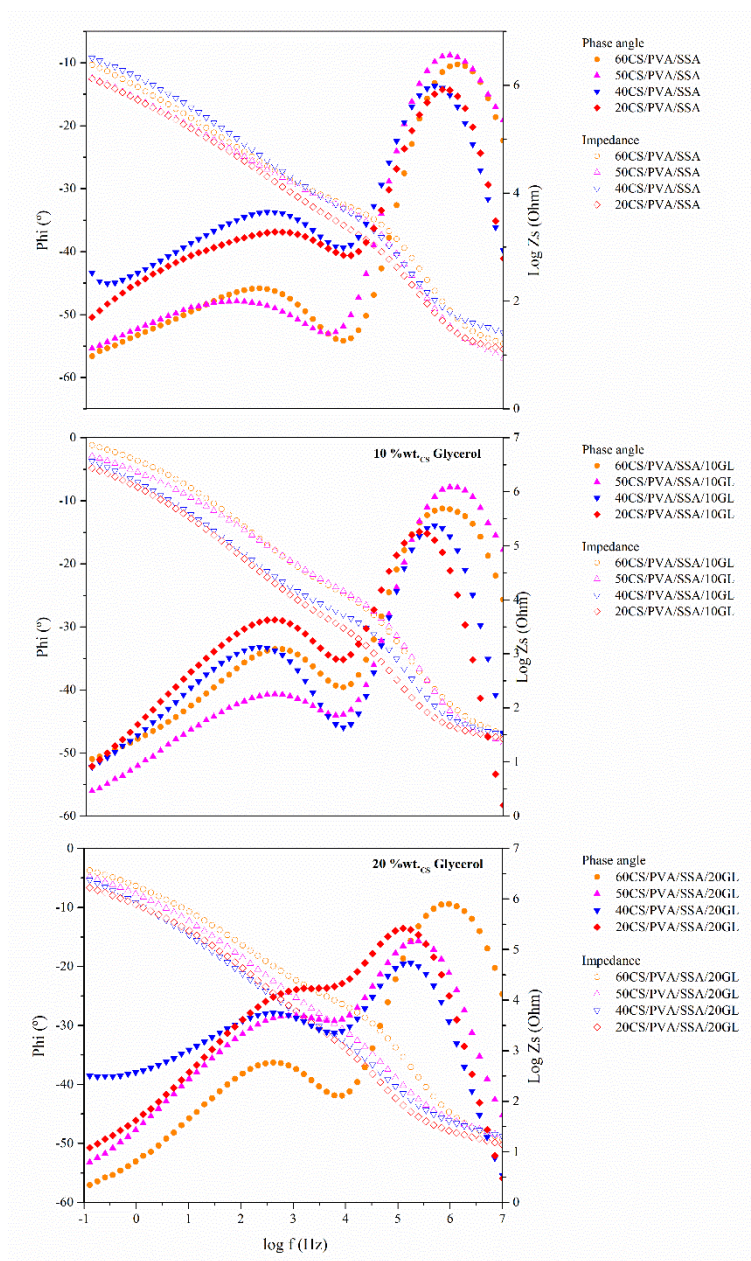


Figure 7. Bode diagram of the pre-hydrated CS/PVA-based polyelectrolytes.

3.4. Direct ethanol fuel cell (DEFC) test

The performance of the crosslinked CS/PVA/SSA-based polyelectrolytes was evaluated in a direct ethanol fuel cell (DEFC) at 20 °C and 2 M ethanol as fuel. Among all the prepared membranes, the 40CS/PVA/SSA and 20CS/PVA/SSA with GL were especially selected for the DEFC test as a proof of concept. They offered the most appropriate balance of flexibility and manageability for the preparation of the membrane electrode assembly (MEA). These membranes do not generate fragile cracks, have a uniform surface to ensure homogeneous conductive behaviour, showed reasonable values of swelling, high diffusion coefficient and adequate proton conductivity.

The polarisation curves of the CS/PVA/SSA/GL membranes in the DEFC were compared to those of Nafion®, measured at the same operating conditions, which results are shown in **Figure 8**. The

obtained values of the maximum power density (P_{max}) and the associated current density (I_{max}) are summarised in **Table 5**.

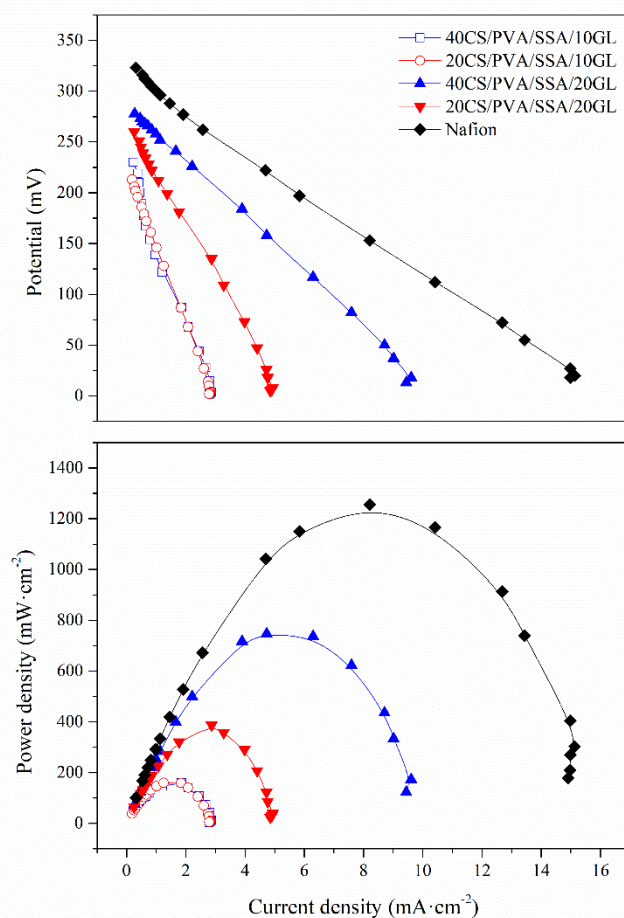


Figure 8. DEFC polarisation curves of the CS/PVA-based polyelectrolytes, in comparison to that of Nafion®, measured at 20 °C and 2 M ethanol as fuel.

According to the results, the power density was strongly influenced by the CS, PVA and GL percentage. The higher the presence of CS and the higher the proportion of GL was in the membrane, the better the behaviour. In particular, promising results were found for the 40CS/PVA/SSA/20GL, with a value of 746.79 $\text{mW}\cdot\text{cm}^{-2}$ and a current density of 4.72 $\text{mA}\cdot\text{cm}^{-2}$. The proposed membranes containing CS, PVA, SSA and GL revealed a compact and interconnected structure, with good manageability, high dimensional and swelling stability along with reasonable proton conductivity that resulted in a suitable performance when tested in the DEFC.

Table 5. Maximum power density (P_{max}) and associated current density (I_{max}) of the crosslinked 40CS/PVA and 20CS/PVA polyelectrolytes containing 10 and 20 %wt.cs of GL, measured at 20 °C and 2 M ethanol as fuel.

Membrane	P_{max} ($\text{mW}\cdot\text{cm}^{-2}$)	I_{max} ($\text{mA}\cdot\text{cm}^{-2}$)
40CS/PVA/SSA/10GL	160.82	1.84
20CS/PVA/SSA/10GL	140.76	1.24
40CS/PVA/SSA/20GL	746.79	4.72
20CS/PVA/SSA/20GL	386.98	2.86

4. Conclusions

Functionalised chitosan/poly(vinyl alcohol)-based polyelectrolytes were obtained by means of their combination with sulfosuccinic acid (SSA) as crosslinking and sulfonating agent, and glycerol (GL) to promote their flexibility and manageability. The combination of solvent-casting and thermal-crosslinking sequence permitted to obtain homogeneous polyelectrolytes with controlled morphology.

The CS/PVA/SSA-based polyelectrolytes generally showed a synergetic increase of the thermo-oxidative stability, absorption capability and diffusion of ethanol, and proton conductivity, in contrast to those of neat CS or crosslinked PVA. The ranges of thermo-oxidative stability –far above 60 °C–, the electrical insulating behaviour –around $10^{-8} \text{ S} \cdot \text{cm}^{-1}$ –, and the ethanol absorption capabilities –between 35% and 60%– were appropriate for the typical service conditions of fuel cells.

Despite the GL reduced the ethanol absorption, the diffusion coefficient and the proton conductivity, it increased the ductile manageability to be mounted on the MEA, reducing the probabilities of fragile breakage.

The crosslinked polyelectrolytes of 40CS/PVA/SSA/20GL, showed the best behaviour in the DEFC test, with a maximum value of and power density of $746 \text{ mW} \cdot \text{cm}^{-2}$. The research to increase the proton conductivity and power of polymeric CS/PVA/SSA-based membranes represent a challenging alternative to current polyelectrolytes for fuel cells, given their intrinsic properties, reasonable cost, non-hazardous behaviour and environmentally friendly attributes.

Acknowledgements

The Spanish Ministry of Economy, Industry and Competitiveness is acknowledged for the projects ENE2017-86711-C3-1-R and UPOV13-3E-1947. The Spanish Ministry of Education, Culture and Sports is thanked for the pre-doctoral FPU grant for O. Gil-Castell (FPU13/01916).

References

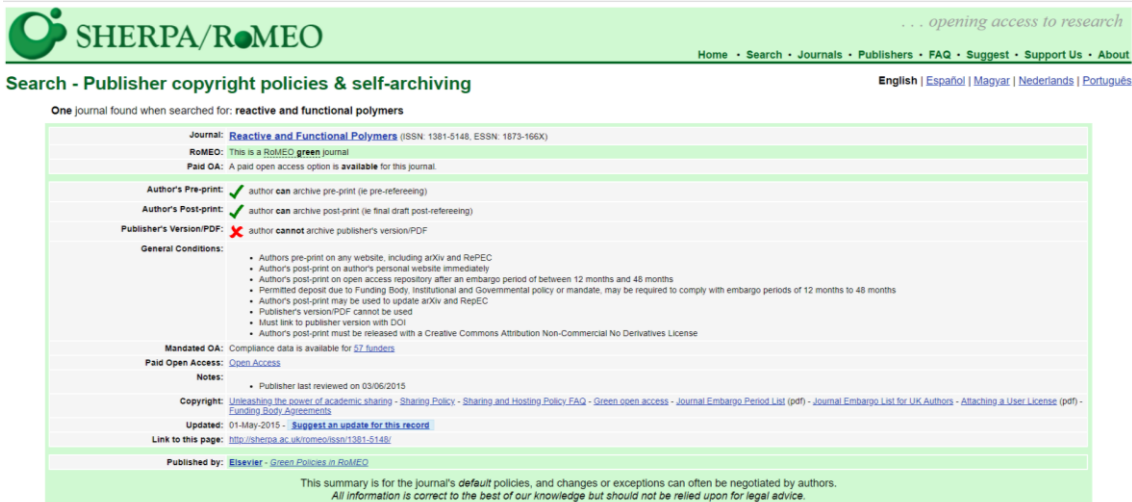
- [1] N. Shaari, S.K. Kamarudin, Chitosan and alginate types of bio-membrane in fuel cell application: An overview, *J. Power Sources*. 289 (2015) 71–80. doi:10.1016/j.jpowsour.2015.04.027.
- [2] H. Vaghari, H. Jafarizadeh-Malmiri, A. Berenjian, N. Anarjan, Recent advances in application of chitosan in fuel cells, *Sustain. Chem. Process.* 1 (2013) 16. doi:10.1186/2043-7129-1-16.
- [3] K. Pourzare, Y. Mansourpanah, S. Farhadi, Advanced nanocomposite membranes for fuel cell applications: a comprehensive review, *Biofuel Res. J.* 3 (2016) 496–513. doi:10.18331/BRJ2016.3.4.4.
- [4] J.D. Badia, O. Gil-Castell, A. Ribes-Greus, Long-term properties and end-of-life of polymers from renewable resources, *Polym. Degrad. Stab.* 137 (2017) 35–57. doi:10.1016/j.polymdegradstab.2017.01.002.
- [5] C. Author, H. Jafarizadeh Malmiri, M. Ali Ghaz Jahanian, A. Berenjian, Potential Applications of Chitosan Nanoparticles as Novel Support in Enzyme Immobilization, *Am. J. Biochem. Biotechnol.* 8203219 (2012) 203–219. doi:10.3844/ajbbsp.
- [6] T. Chakrabarty, M. Kumar, V. Shahi, Chitosan Based Membranes for Separation, Pervaporation and Fuel Cell Applications: Recent Developments, *Biopolymers*. (2010) 5–8. doi:10.5772/10263.
- [7] J. Ma, Y. Sahai, Chitosan biopolymer for fuel cell applications, *Carbohydr. Polym.* 92 (2013) 955–975. doi:10.1016/j.carbpol.2012.10.015.
- [8] V. Zargar, M. Asghari, A. Dashti, A Review on Chitin and Chitosan Polymers: Structure, Chemistry, Solubility, Derivatives, and Applications, *ChemBioEng Rev.* 2 (2015) 204–226. doi:10.1002/cben.201400025.
- [9] P. Mukoma, B.R. Jooste, H.C.M. Vosloo, A comparison of methanol permeability in Chitosan and Nafion 117 membranes at high to medium methanol concentrations, *J. Memb. Sci.* 243 (2004) 293–299. doi:10.1016/j.memsci.2004.06.032.
- [10] P. Mukoma, B.R. Jooste, H.C.M. Vosloo, Synthesis and characterization of cross-linked chitosan membranes for application as alternative proton exchange membrane materials in fuel cells, *J. Power Sources*. 136 (2004) 16–23. doi:10.1016/j.jpowsour.2004.05.027.
- [11] B. Ma, C. Qin, A. Li, X. Zhao, X. He, Structure and properties of chitin whisker reinforced chitosan membranes, *Int. J. Biol. Macromol.* 64 (2014) 341–346. doi:10.1016/j.ijbiomac.2013.12.015.
- [12] E. Dashtimoghadam, M.M. Hasani-Sadrabadi, H. Moaddel, Structural modification of chitosan biopolymer as a novel

- polyelectrolyte membrane for green power generation, *Polym. Adv. Technol.* 21 (2010) 726–734. doi:10.1002/pat.1496.
- [13] B. Smitha, S. Sridhar, A.A. Khan, Polyelectrolyte complexes of chitosan and poly(acrylic acid) as proton exchange membranes for fuel cells, *Macromolecules.* 37 (2004) 2233–2239. doi:10.1021/ma0355913.
- [14] B. Smitha, S. Sridhar, A.A. Khan, Synthesis and characterization of poly(vinyl alcohol)-based membranes for direct methanol fuel cell, *J. Appl. Polym. Sci.* 95 (2005) 1154–1163. doi:10.1002/app.20982.
- [15] S. Meenakshi, S.D. Bhat, A.K. Sahu, P. Sridhar, S. Pitchumani, A.K. Shukla, Chitosan-polyvinyl alcohol-sulfonated polyethersulfone mixed-matrix membranes as methanol-barrier electrolytes for DMFCs, *J. Appl. Polym. Sci.* 124 (2012) E73–E82. doi:10.1002/app.35522.
- [16] A.C. Dupuis, Proton exchange membranes for fuel cells operated at medium temperatures: Materials and experimental techniques, *Prog. Mater. Sci.* 56 (2011) 289–327. doi:10.1016/j.pmatsci.2010.11.001.
- [17] M.H. Buraidah, A.K. Arof, Characterization of chitosan/PVA blended electrolyte doped with NH₄I, *J. Non. Cryst. Solids.* 357 (2011) 3261–3266. doi:10.1016/j.jnoncrysol.2011.05.021.
- [18] K. Lewandowska, Miscibility and thermal stability of poly(vinyl alcohol)/chitosan mixtures, *Thermochim. Acta.* 493 (2009) 42–48. doi:10.1016/j.tca.2009.04.003.
- [19] S.J. Peighambaroust, S. Rowshanzamir, M. Amjadi, Review of the proton exchange membranes for fuel cell applications, Elsevier Ltd, 2010. doi:10.1016/j.ijhydene.2010.05.017.
- [20] I.R. Rodrigues, M.M. de Camargo Forte, D.S. Azambuja, K.R.L. Castagno, Synthesis and characterization of hybrid polymeric networks (HPN) based on polyvinyl alcohol/chitosan, *React. Funct. Polym.* 67 (2007) 708–715. doi:10.1016/J.REACTFUNCTPOLYM.2007.05.010.
- [21] M.A. Witt, G.M.O. Barra, J.R. Bertolino, A.T.N. Pires, Crosslinked chitosan/poly (vinyl alcohol) blends with proton conductivity characteristic, *J. Braz. Chem. Soc.* 21 (2010) 1692–1698. doi:10.1590/S0103-50532010000900014.
- [22] O. Gil-Castell, Development, characterisation and validation of functionalised polymer-based materials for smart applications, Universitat Politècnica de València, 2018. doi:10.4995/Thesis/10251/107950.
- [23] P. Neogi, *Diffusion in polymers*, Marcel Dekker, New York, 1996.
- [24] X. Qian, N. Gu, Z. Cheng, X. Yang, E. Wang, S. Dong, Methods to study the ionic conductivity of polymeric electrolytes using a.c. impedance spectroscopy, *J. Solid State Electrochem.* 6 (2001) 8–15. doi:10.1007/s100080000190.
- [25] B. Ma, X. Li, A. Qin, C. He, A comparative study on the chitosan membranes prepared from glycine hydrochloride and acetic acid, *Carbohydr. Polym.* 91 (2013) 477–482. doi:10.1016/j.carbpol.2012.07.081.
- [26] M. Fernandes Queiroz, K. Melo, D. Sabry, G. Sassaki, H. Rocha, Does the Use of Chitosan Contribute to Oxalate Kidney Stone Formation?, *Mar. Drugs.* 13 (2014) 141–158. doi:10.3390/md13010141.
- [27] M.S. Boroglu, S. Cavus, I. Boza, A. Ata, Synthesis and characterization of poly(vinyl alcohol) proton exchange membranes modified with 4,4-diaminodiphenylether-2,2-disulfonic acid, *Express Polym. Lett.* 5 (2011) 470–478. doi:10.3144/expresspolymlett.2011.45.
- [28] J. Ming Yang, H. Chih Chiu, Preparation and characterization of polyvinyl alcohol/chitosan blended membrane for alkaline direct methanol fuel cells, *J. Memb. Sci.* 419–420 (2012) 65–71. doi:10.1016/j.memsci.2012.06.051.
- [29] C. Pradal, P. Kithva, D. Martin, M. Trau, L. Grøndahl, Improvement of the wet tensile properties of nanostructured hydroxyapatite and chitosan biocomposite films through hydrophobic modification, *J. Mater. Chem.* 21 (2011) 2330–2337. doi:10.1039/c0jm03080e.
- [30] A. Jokar, M.H. Azizi, Z. Hamidi Esfehiani, The Interaction Effects of Montmorillonite and Glycerol on the Properties of Polyvinyl Alcohol-montmorillonite Films, *Nutr. Food Sci. Res.* 4 (2017) 25–34. doi:10.18869/acadpub.nfsr.4.2.4.
- [31] S.C.M. Fernandes, C.S.R. Freire, A.J.D. Silvestre, C. Pascoal Neto, A. Gandini, L.A. Berglund, L. Salmén, Transparent chitosan films reinforced with a high content of nanofibrillated cellulose, *Carbohydr. Polym.* 81 (2010) 394–401. doi:10.1016/J.CARBPOL.2010.02.037.
- [32] S.C.M. Fernandes, L. Oliveira, C.S.R. Freire, A.J.D. Silvestre, C.P. Neto, A. Gandini, J. Desbrières, Novel transparent nanocomposite films based on chitosan and bacterial cellulose, *Green Chem.* 11 (2009) 2023. doi:10.1039/b919112g.
- [33] A. Martínez-Felipe, C. Moliner-Estopinan, C.T. Imrie, A. Ribes-Greus, Characterization of Crosslinked Poly(vinyl alcohol)-Based Membranes with Different Hydrolysis Degrees for Their Use as Electrolytes in Direct Methanol Fuel Cells, *Polym. Polym. Compos.* 21 (2013) 449–456. doi:10.1002/app.
- [34] A. Gómez-Siurana, A. Marcilla, M. Beltrán, D. Berenguer, I. Martínez-Castellanos, S. Menargues, TGA/FTIR study of tobacco and glycerol-tobacco mixtures, *Thermochim. Acta.* 573 (2013) 146–157. doi:10.1016/j.tca.2013.09.007.
- [35] J.M. Morancho, J.M. Salla, A. Cadenato, X. Fernández-Francos, X. Ramis, P. Colomer, Y. Calventus, R. Ruíz, Kinetic studies of the degradation of poly(vinyl alcohol)-based proton-conducting membranes at low temperatures, *Thermochim. Acta.* 521 (2011) 139–147. doi:10.1016/j.tca.2011.04.016.
- [36] M. Mohsin, A. Hossin, Y. Haik, Thermal and Mechanical Properties of Poly(vinyl alcohol) Plasticized with Glycerol, *J Appl Polym Sci.* 122 (2011) 3102–3109. doi:10.1002/app.34229.
- [37] M. Gurgel, M. Altenhofen, L. Oliveira, M.M. Beppu, Natural-based plasticizers and biopolymer films, *Eur. Polym. J.* 47 (2011) 254–263. doi:10.1016/j.eurpolymj.2010.12.011.
- [38] E. Bakanura, L. Wu, L. Ge, Z. Yang, T. Xu, Mixed matrix proton exchange membranes for fuel cells: state of the art and perspectives Mixed matrix proton exchange membranes for fuel cells: state of the art and perspectives, *Prog. Polym. Sci.* 57 (2015) 103–152. doi:10.1016/j.progpolymsci.2015.11.004.
- [39] J. Zhang, J. Wu, H. Zhang, PEM Fuel Cell Testing and Diagnosis, Elsevier Science, 2013. doi:10.1016/B978-0-444-53688-4.00005-X.
- [40] B. Emonts, L. Blum, T. Grube, W. Lehnert, J. Mergel, M. Müller, R. Peters, Technical Advancement of Fuel-Cell Research and Development, in: *Fuel Cell Sci. Eng.*, Wiley-VCH Verlag GmbH & Co. KGaA, Weinheim, Germany, 2012: pp. 1–42. doi:10.1002/9783527650248.ch1.
- [41] O. Gil-Castell, J.D. Badia, T. Kittikorn, E. Strömberg, A. Martínez-Felipe, M. Ek, S. Karlsson, A. Ribes-Greus, Hydrothermal ageing of polylactide/sisal biocomposites. Studies of water absorption behaviour and Physico-Chemical performance, *Polym. Degrad. Stab.* 108 (2014) 212–222. doi:10.1016/j.polymdegradstab.2014.06.010.

O. Gil-Castell, R. Teruel-Juanes, F. Arenga, A. M. Salaberria, M. G. Baschetti, J. Labidi, J. D. Badia, A. Ribes-Greus. Crosslinked chitosan/poly(vinyl alcohol)-based polyelectrolytes for proton exchange membranes. *Reactive and Functional Polymers* 2019:142:213-222

- [42] J.D. Badia, L. Santonja-Blasco, A. Martínez-Felipe, A. Ribes-Greus, Hygrothermal ageing of reprocessed polylactide, *Polym. Degrad. Stab.* 97 (2012) 1881–1890. doi:10.1016/j.polymdegradstab.2012.06.001.
- [43] C. González-Guisasola, A. Ribes-Greus, Dielectric relaxations and conductivity of cross-linked PVA/SSA/GO composite membranes for fuel cells, *Polym. Test.* 67 (2018) 55–67. doi:10.1016/j.polymertesting.2018.01.024.
- [44] I. Shabani, M.M. Hasani-Sadrabadi, V. Haddadi-Asl, M. Soleimani, Nanofiber-based polyelectrolytes as novel membranes for fuel cell applications, *J. Memb. Sci.* 368 (2011) 233–240. doi:10.1016/J.MEMSCI.2010.11.048.
- [45] V. V. Binsu, R.K. Nagarale, V.K. Shahi, P.K. Ghosh, Studies on N-methylene phosphonic chitosan/poly(vinyl alcohol) composite proton-exchange membrane, *React. Funct. Polym.* 66 (2006) 1619–1629. doi:10.1016/j.reactfunctpolym.2006.06.003.

ANNEX. OPEN-ACCESS POLICIES



The screenshot displays the SHERPA/RoMEO website interface. At the top, the SHERPA/RoMEO logo is on the left, and the tagline "... opening access to research" is on the right. Below the logo, navigation links for Home, Search, Journals, Publishers, FAQ, Suggest, Support Us, and About are visible. The main heading is "Search - Publisher copyright policies & self-archiving", with language options for English, Español, Magyar, Nederlands, and Português. The search results show one journal found for the query "reactive and functional polymers": "Reactive and Functional Polymers" (ISSN: 1381-5148, EISSN: 1873-166X). The journal is categorized as a RoMEO green journal, and a paid open access option is available. The archiving policies are as follows: Author's Pre-print: author can archive pre-print (ie pre-refereeing); Author's Post-print: author can archive post-print (ie final draft post-refereeing); Publisher's Version/PDF: author cannot archive publisher's version/PDF. General conditions include: Authors pre-print on any website, including arXiv and RePEc; Author's post-print on author's personal website immediately; Author's post-print on open access repository after an embargo period of between 12 months and 48 months; Permitted deposit due to Funding Body, Institutional and Governmental policy or mandate, may be required to comply with embargo periods of 12 months to 48 months; Author's post-print may be used to update arXiv and RePEc; Publisher's version/PDF cannot be used; Must link to publisher version with DOI; Author's post-print must be released with a Creative Commons Attribution Non-Commercial No Derivatives License. Mandated OA: Compliance data is available for 67 funders. Paid Open Access: Open Access. Notes: Publisher last reviewed on 03/06/2015. Copyright: Users share the power of academic sharing - Sharing Policy - Sharing and Hosting Policy FAQ - Green open access - Journal Embargo Period List (pdf) - Journal Embargo List for UK Authors - Attaching a User License (pdf) - Funding Body Approvals. Updated: 01-May-2015 - Suggest an update for this record. Link to this page: http://sherpa.ac.uk/romeo/issn/1381-5148/. Published by: Elsevier - Green Policies in RoMEO. A disclaimer at the bottom states: "This summary is for the journal's default policies, and changes or exceptions can often be negotiated by authors. All information is correct to the best of our knowledge but should not be relied upon for legal advice."